Transition Effects on Airfoil Dynamics and the Implications for Subscale Tests

L.E. Ericsson*
Lockheed Missiles & Space Company, Inc., Sunnyvale, California

Experimental results showing the effect of boundary-layer transition on airfoil unsteady aerodynamics are analyzed. It is found that boundary-layer transition can have a significant effect even in the case of attached flow. The problem this causes in regard to the use of wind tunnel test results is discussed.

Nomenclature

A = disturbance amplitude
A_1 = disturbance amplitude in freestream
A_o = initial disturbance amplitude in boundary layer
A_r = reference initial disturbance amplitude in boundary layer at $M_r(=1.3)$
c = airfoil chord
$\bar{c}$ = mean aerodynamic chord
D = drag, coefficient $C_D = D/(\rho_\infty U_\infty^2/2)S$
f = frequency
K = proportionality constant, Eq. (1)
L = lift, coefficient $C_L = L/(\rho_\infty U_\infty^2/2)S$
l = sectional lift, coefficient $c_1 = 1/(\rho_\infty U_\infty^2/2)c$
M = Mach number
m = mass flow injected
m_b = calculated mass flow in boundary layer just upstream of air holes
m_p = sectional pitching moment, coefficient $c_m = m_p/(\rho_\infty U_\infty^2/2)c^2$
P = static pressure, coefficient $C_p = (P - P_\infty)/(\rho_\infty U_\infty^2/2)$
p = rotation rate
Re = Reynolds number, $= U_\infty c/\nu_\infty$ or $= U_\infty \bar{c}/\nu_\infty$
S = wing area
t = time
Δt = time lag
U = velocity
x = chordwise distance from leading edge
z = vertical translation, positive downward
α = angle of attack
$\bar{\alpha}$ = effective angle of attack, $= \alpha_o + \theta + \dot{z}/U_\infty$
α_o = trim angle of attack
Δ = increment and amplitude
ϵ = rms wing root strain
θ = perturbation in pitch
Λ = leading edge sweep
ν = kinematic viscosity
ξ = dimensionless x coordinate, $= x/c$
ρ = air density
ϕ = phase lag, $= \Delta\psi = \omega\Delta t$
ψ = phase angle, $\psi = \omega t$
$\omega, \bar{\omega}$ = angular frequency, $\omega = 2\pi f$, $\bar{\omega} = \omega c/U_\infty$ or $= \omega\bar{c}/U_\infty$

Subscripts

C = convection
LE = leading edge
O = oscillation center
r = reference
s = separation or stall
tr = transition
W = wall
w = wake
o = initial or time-average value
$1,\infty$ = freestream conditions

Superscripts

i = transition-induced, e.g. $\Delta^i C_l$ in Fig. 10

Derivative Symbols

$\dot{\theta}$ = $\partial\theta/\partial t$; $\ddot{z} = \partial^2 z/\partial t^2$

Introduction

IT was recently demonstrated[1] that simulation of the full scale Reynolds number is not only important when extensive flow separation regions are present[2] but also in the case of attached flow. In an aeroelastic test at $\alpha = 0$ of a 25 deg swept wing, with a symmetric airfoil section,[1] violent oscillations in the first bending mode occurred if the location of boundary-layer transition was not fixed (Fig. 1). The oscillations were of the limit cycle type, caused by initially negative total (aerodynamic plus structural) damping (Fig. 2). Similar results have been obtained by others[3] when transition is not fixed.

Large effects of transition are also observed on airfoil sections with attached flow in torsional oscillations,[4] rather than plunging oscillations.[1,3] However, the flow mechanisms through which the coupling between vehicle motion and boundary layer transition occurs are very different in the two cases, as will be shown.

In neither case can the quasisteady flow mechanism described in Ref. 1 explain the effect of transition on the airfoil unsteady aerodynamics,[5] contrary to the author's claim.[1]

Analytic Approach

The analysis is based on the following basic assumptions:

1) The effect of the pressure gradient impressed upon the boundary layer is very similar in the case of transition and flow separation, e.g., the increase of the adversity of the pressure gradient, when the static angle of attack is increased, causes both transition and separation to occur earlier (closer to the leading edge) in the leeside flow of an airfoil.

2) The airfoil oscillation is too slow to interact with the transition process itself; it only changes the ambient pressure gradient and the boundary-layer development, profile, thick-

Presented as Paper 87-2353 at the AIAA 5th Applied Aerodynamics Conference, Monterey, CA, Aug. 17-19, 1987; received Feb. 5, 1988; revision received May 15, 1989.

*Senior Consulting Engineer. Fellow AIAA.

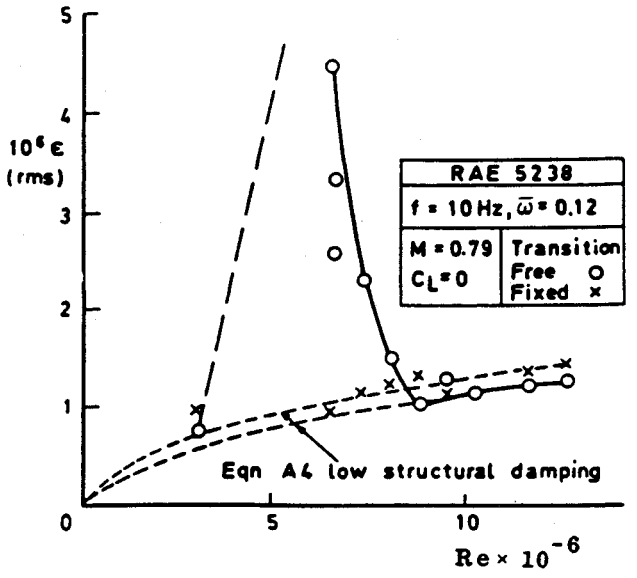

Fig. 1 Variation of unsteady wing-root strain with Reynolds number.[1]

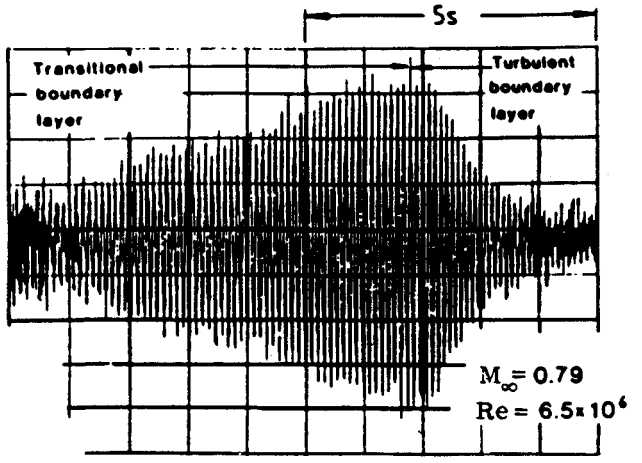

Fig. 2 Typical response of wing-tip accelerometer.[1]

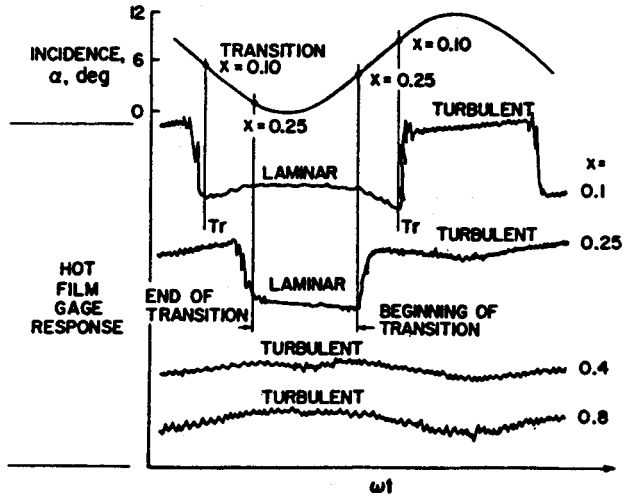

Fig. 3 Skin friction measurements on pitching airfoil.[7]

ness, etc., via surface perturbations. (e.g., the leading-edge-jet effect illustrated in Fig. 6, to be discussed later.)

Thus, the airfoil oscillation affects the boundary-layer transition through the same basic flow mechanism it affects dynamic stall.

That the effect of the airfoil pitching motion on boundary-layer transition in attached flow is very similar to that on dynamic stall[6] has been demonstrated[7] (Fig. 3). Just as in the case of boundary-layer separation, the transition is delayed on the pitching "upstroke" and promoted on the "downstroke." Thus, it will be assumed in the present analysis that the unsteady flow concepts developed for dynamic stall analysis[8-10] can be applied to describe the effect of transition on the unsteady airfoil aerodynamics.

Analysis

Using the unsteady flow concepts developed in Refs. 8-10, the coupling between boundary-layer transition and airfoil oscillations in pitch and plunge will be analyzed.

Pitching Oscillations

Greidanus et al.,[4] performing a thorough experimental check of existing theory for small amplitude oscillations at $\alpha = 0$, obtained results that illustrate the dynamic effect of the strong coupling existing between the airfoil motion and boundary-layer transition (Fig. 4). Their model, a 7.3% thick symmetrical airfoil, had natural boundary-layer transition occurring on it, if no tripping was used.

When natural boundary-layer transition is permitted to occur near the trailing edge, there are drastic variations from the expected theoretical trends, the latter being in agreement with the trip-on experimental results[4] (Fig. 4). The oscillation center, $\xi_o = 0.227$, is close to the 25% chord, where attached flow lift has no effect on the pitching moment. That is the reason for the large effects of trailing-edge transition. Figure 5 explains what happens.[11] The reduced frequency was changed by changing the (incompressible flow) velocity, keeping the pitching frequency constant. Thus, the velocity, and hence the Reynolds number, increases with decreasing reduced frequency. As a consequence, transition moves forward from the trailing edge with decreasing reduced frequency $\bar{\omega}$.

At angle of attack, the boundary-layer transition occurs more forward on the leeward side, mainly due to the increased adverse pressure gradient. The differential transition on top and bottom surfaces causes a force couple (Fig. 5, insets), similar to what is the result of trailing-edge separation. When the Reynolds number is increased (decreasing $\bar{\omega}$), the transition moves forward. Thus, the forward force component loses lever arm and becomes less and less effective, causing the overall static effect of boundary-layer transition to change from destabilizing to stabilizing. With this in mind, one can illustrate the effects, using vector diagrams, as shown in Fig. 5.

In the frequency range $0.8 < \bar{\omega} < 1.2$, the transition takes place near the trailing edge, causing the moment increment of magnitude $\Delta|c_m|_{tr_1}$. Note that the stabilizing moment $(-c_m)$ is used in the vector diagram in sign agreement with the way the experimental results were presented in Ref. 4. In absence of the effects of free transition, the moment vector leads the velocity vector by $-\psi \approx 80$ deg (due to the high apparent mass effect at these high-reduced frequencies). Without any motion-induced lag effects, the instantaneous transition-induced moment would lead the angle-of-attack vector, $\theta(t)$, by 180 deg, as it is destabilizing.

Using the flow concepts discussed in Refs. 8-10 for dynamic stall, the time lag effects will be estimated. That is, Eq. (18) in Ref. 9 is used with $\alpha = \alpha_s = 0$. For the frequency range of interest, one obtains $\bar{\omega}\Delta\theta$ deg < 0.02 for the oscillation amplitude ($\Delta\theta < 1$ deg) used in the experiment[4] (Fig. 4). Thus, Eq.

(18a) in Ref. 9 applies:

$$(\omega t)_{LE} = 2\tan^{-1}\left\{\left[\frac{\cos(\phi_w+\phi_s)}{K\bar{\omega}+\sin(\phi_w+\phi_s)}\right]\left\{\sqrt{1+\left[\frac{K\bar{\omega}+\sin(\phi_w+\phi_s)}{\cos(\phi_w+\phi_s)}\right]^2}-1\right\}\right\} \quad (1)$$

When transition occurs near the leading edge, $(\omega t)_{LE} = (\omega t)_{tr}$ is obtained directly from Eq. (1) with $\phi = 14$ deg, the attached flow value for $\bar{\omega} > 0.16$, and $\phi_s = 0.75\bar{\omega}$, the turbulent value.[9] When transition occurs near the trailing edge, $(\omega t)_{tr}$ is obtained as

$$(\omega t)_{tr} = (\omega t)_{LE} + \phi_c \quad (2)$$

where $(\omega t)_{LE}$ is obtained from Eq. (1) with $\phi_s = 0$. From Ref. 9, one obtains $\phi_C = 1.25\,\xi_{tr}\bar{\omega}$, and $K = 2.91$ for $\xi_o = 0.227$.

The transition effects in Fig. 5 appear to have started at $\bar{\omega} \approx 1.6$; $\xi_{tr} \approx 1$ being the associated parameter value. In the region of negligible pressure gradients upstream of the trailing edge, one can assume that ξ_{tr} is inversely proportional to the Reynolds number and, thereby, to the velocity U_∞. Thus, one would expect transition to occur at $\xi_{tr} \approx 0.5$ when $\bar{\omega} \approx 0.8$. For those two cases, $\Delta\psi_1$ in Fig. 5 is computed from Eqs. (1) and (2) to be 182 deg and 98 deg, respectively. These values are in good agreement with the experimental results. At $\bar{\omega} \approx 1.6$, the value $\Delta\phi_1 = 182$ deg would result in $\Delta\psi_1 \approx 0$, whereas close to the maximum $\Delta\psi_1$ should result for $\Delta\phi_1 = 98$ deg, all in agreement with the experimental results in Fig. 5. At $\bar{\omega} \approx 1.6$, the combined vector $|c_m + \Delta c_{mtr}|$ is definitely less than $|c_m|$ in agreement with the experiment.[4] At $\bar{\omega} \approx 0.8$, $|c_m + \Delta c_{mtr}|$ is larger than $|c_m|$. Thus, at some value $\bar{\omega} > 0.8$, the two vectors will have the same magnitude, which is also in agreement with the experimental results (Fig. 5).

At $\bar{\omega} = 0.6$, transition has apparently moved to the oscillation center ($\Delta\psi = 0$ in Fig. 5), and for $\bar{\omega} < 0.6$ the transition-induced moment becomes statically stabilizing (see top sketch in Fig. 5). In this case, when transition occurs near the leading edge, one neglects any convective time lag effects, i.e., $\phi_C = 0$. Equation (1) gives a phase lag $\Delta\phi_2$ that decreases from 72.5

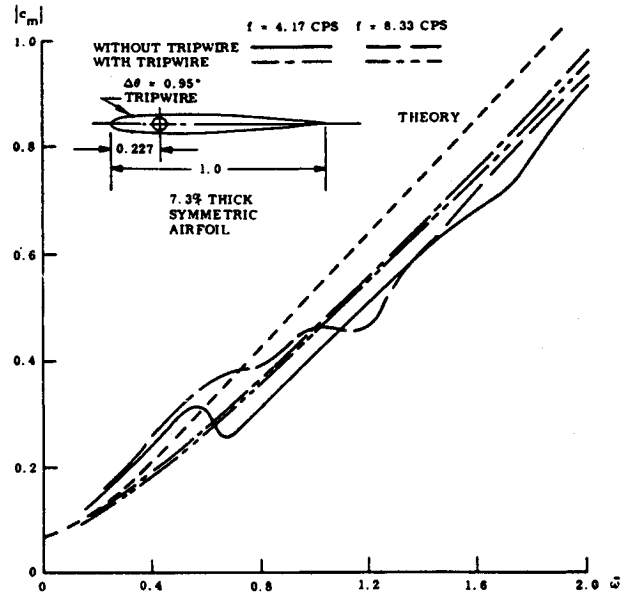

a) Moment-amplitude variation with frequency

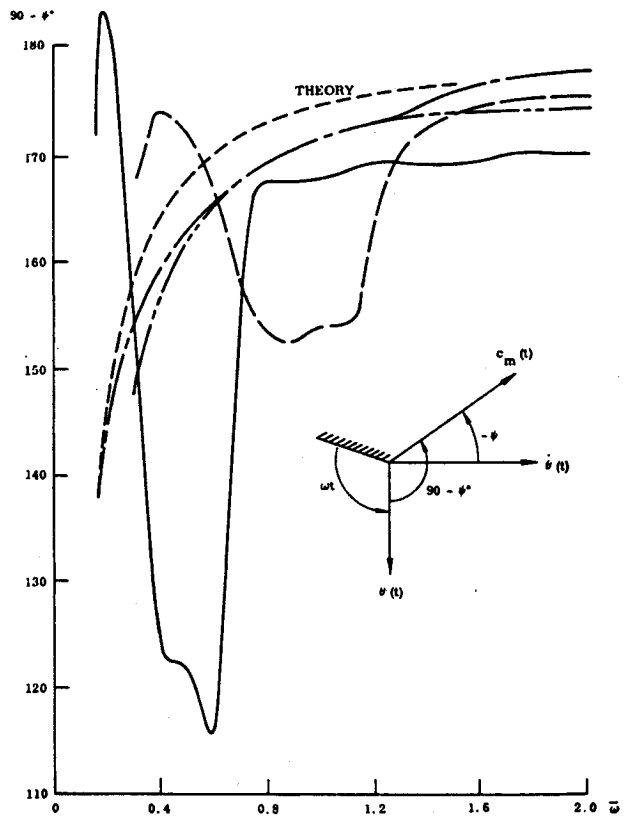

b) Phase-lead variation with frequency

Fig. 4 Effect of trip wire on dynamic airfoil characteristics.[4]

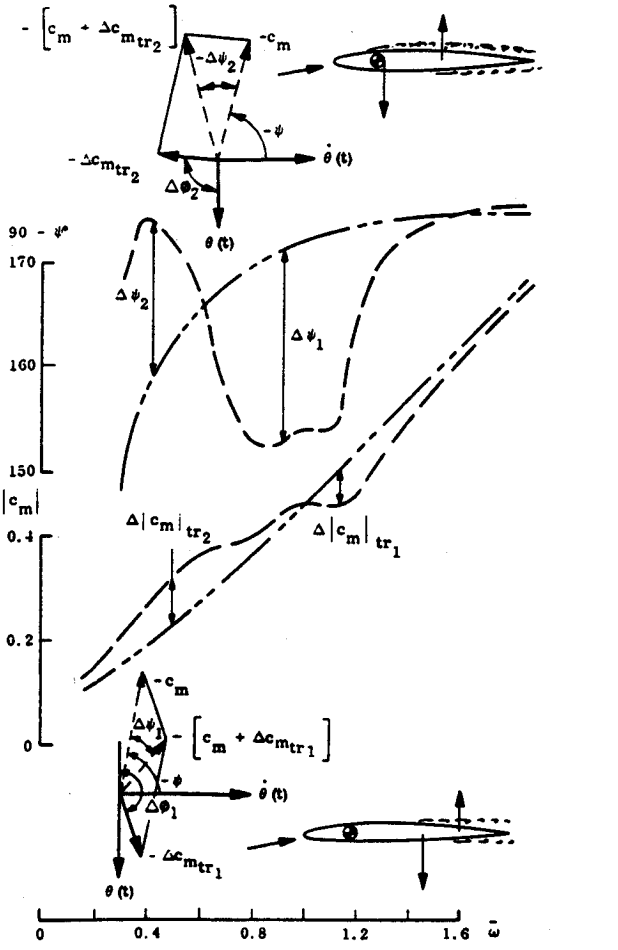

Fig. 5 Effect of transition-induced loads on unsteady aerodynamic characteristics.[10]

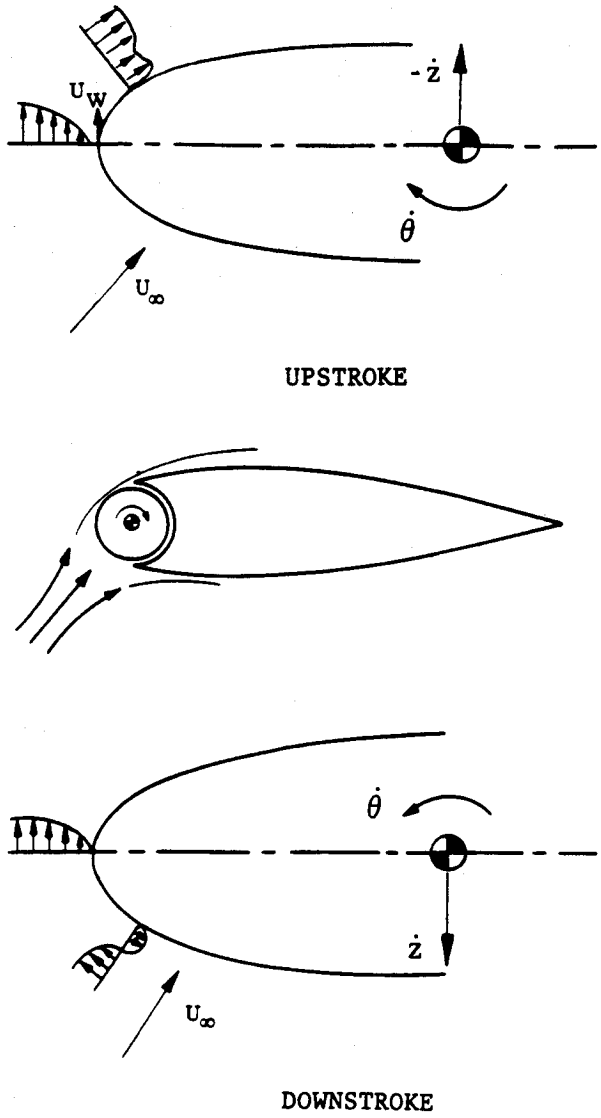

Fig. 6 Leading-edge-jet effect.

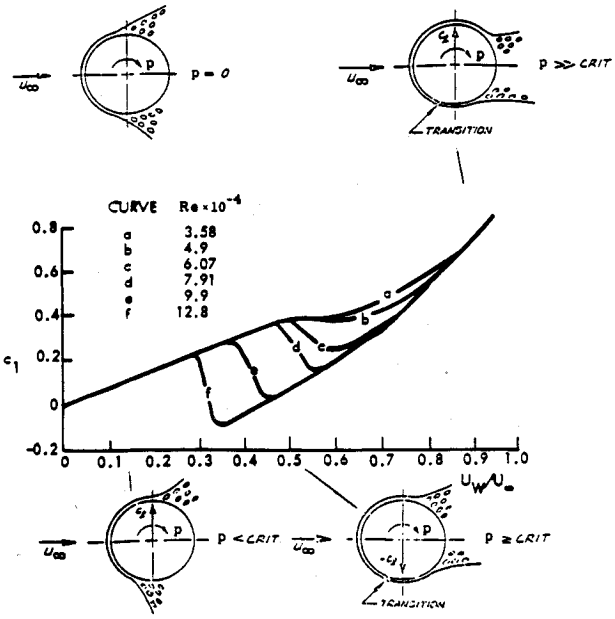

Fig. 7 Magnus lift characteristics for initially subcritical flow conditions.

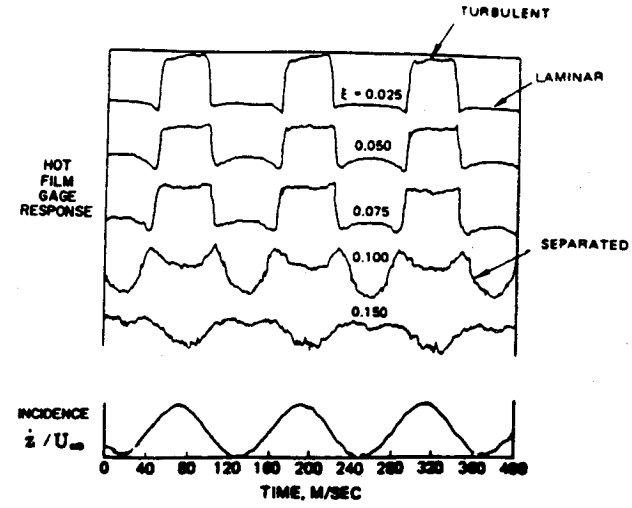

a) Plunging

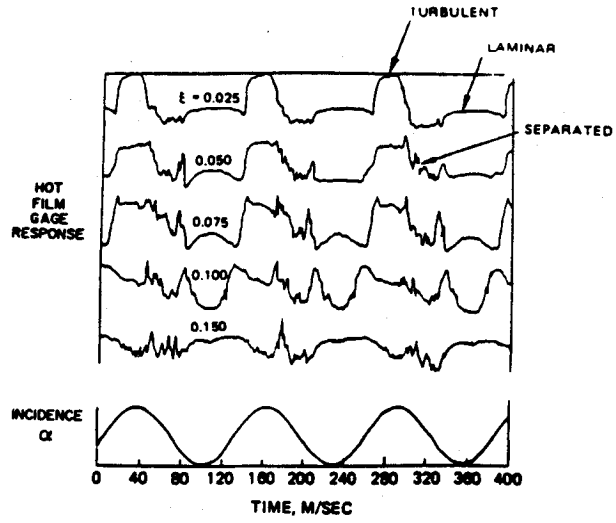

b) Pitching

Fig. 8 Hot film response for plunging and pitching oscillations of a NACA 0012 airfoil.[14]

deg to 47.5 deg when $\bar{\omega}$ is decreased from $\bar{\omega} = 0.4$ to 0.2. This gives a decreasing $\Delta\psi_2$ trend and a combined vector that is of larger magnitude than $|c_m|$, all in agreement with the experimental results in Fig. 5.

For the other test run in Fig. 4, with half the frequency, $f = 4.1$ CPS, the whole interaction is moved down to half the $\bar{\omega}$ values existing for $f = 8.33$ CPS.

Plunging Oscillations

In the case of the pitch oscillations just discussed, accelerated flow and moving wall effects act together to delay boundary-layer transition or separation.[8-10] One effect—the delay due to a less adverse upstream pressure gradient time history and the accelerated flow effect—is the same regardless of whether the angle of attack increase is accomplished by pitching or plunging. The moving wall effect,[12] however, is opposite in the two cases, as is illustrated in Fig. 6. That is, when the angle of attack due to plunging, $\dot{z}/U_\infty$, increases, the moving wall or leading-edge-jet effect[10] on the flow separation or transition is adverse, promoting rather than delaying the occurence of both.

How the moving wall effect influences flow separation and transition is well illustrated by Magnus lift measurements on a rotating circular cylinder[13] (Fig. 7). The positive Magnus lift, at

$U_W/U_\infty < 0.3$, is caused by the wall-jet-like downstream moving wall effect on the top side, which fills out the boundary-layer velocity profile, thereby delaying flow separation. A similar lift contribution is obtained from the upstream moving wall effect on the bottom side, which promotes separation. At $Re = 0.128 \times 10^6$, the so-called Magnus lift reversal occurs for $U_W/U_\infty > 0.3$. This is caused by the upstream moving wall effect on the bottom side, which when the critical U_W/U_∞ – Reynolds number combination is approached, will cause boundary-layer transition to occur upstream of flow separation, thereby changing the separation from the subcritical towards the supercritical type. This results in a more or less discontinuous loss of lift.

The moving wall effect is of significant magnitude only in the region near the stagnation point, where the boundary layer is thin and, therefore, very sensitive to this wall-jet-like action. Carta's hot film response data[14] (Fig. 8) [the amplitudes of $\dot{z}(t)/U_\infty$ and $\theta(t)$ are of the same magnitude] show how the adverse (upstream) moving wall effect $\dot{z}(t)$ promotes transition and causes the plunging airfoil to have a longer run of attached turbulent flow prior to stall. As a result, the flow stays attached past 7.5% chord, whereas flow separation occurs forward of 5% chord on the pitching airfoil, which has a shorter turbulent run before stall due to the opposite, transition-delaying, moving wall effect. In addition to showing the opposite moving wall effects for pitching and plunging oscillations, Fig. 8 also demonstrates that the moving wall effect completely dominates over the effect of the lessened pressure gradient adversity, which is the same for pitching and plunging oscillations. This dominance is found in numerous flow situations both in two-dimensional and three-dimensional flows.[12]

In addition to this motion-induced improvement (or degradation) of the boundary-layer characteristics, there is the convective time lag effect, as was illustrated in the case of the pitching airfoil discussed earlier (Figs. 4 and 5). In the case of plunging oscillations, or bending oscillations of wings that are not highly swept, the time lag effect on the aerodynamics is determined by $\dot{z}(t-\Delta t)/U_\infty$, which, for small amplitude/low-frequency oscillations, such as the ones discussed in Ref. 1, can be Taylor-expanded to yield

$$\dot{z}(t-\Delta t)/U_\infty = \dot{z}(t)/U_\infty - \Delta t\ddot{z}(t)/U_\infty + \ \ldots \qquad (3)$$

That is, the time lag associated with the transition response to a change of the effective angle of attack, $\bar{\alpha} = \dot{z}/U_\infty$, cannot affect the damping (the $\dot{z}$-term) contrary to what is the case for torsional oscillations, where the effective angle of attack is

$$\alpha(t-\Delta t) = \alpha_o + \theta(t) - \Delta t\dot{\theta}(t) \qquad (4)$$

The effect of $\dot{z}(t)/U_\infty$ on the airfoil, with its positive lift slope, $c_{l\alpha} > 0$, is, of course, damping. It is true that the effect of free transition is to generate a negative component, $\Delta c_{l\alpha_{tr}} < 0$. However, it only reduces the magnitude of the (net) positive lift slope. Consequently, the quasisteady flow mechanism described in Ref. 1 cannot generate negative aerodynamic damping. That can only be generated by the moving-wall/leading-edge-jet effect discussed earlier. How strong this effect can be is demonstrated by Carta's data[14] (Fig. 8). As $|\dot{z}|/U_\infty = |\theta|$, the $c_{l\alpha}$ effect is the same for plunging and pitching oscillations. Thus, the data in Fig. 8 indicate that the magnitude of the leading-edge-jet effect is more than enough to completely cancel the $c_{l\alpha}$ effect for the plunging airfoil.

Transition Effects on Bending Oscillations

The plunging airfoil section for the bending wing[1] will experience a transition-promoting moving wall effect on the top side during the "down-stroke" of the bending oscillation. On the bottom side, the moving wall effect is the opposite, delaying transition. As a result, a negative lift component is generated, which drives the oscillation (Fig. 9).

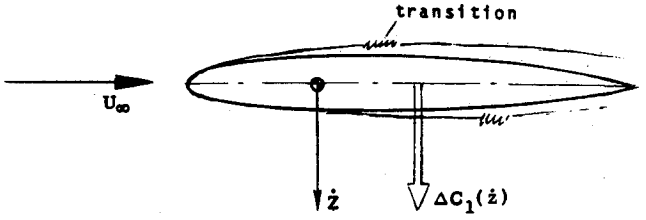

Fig. 9 Transition-induced loads.

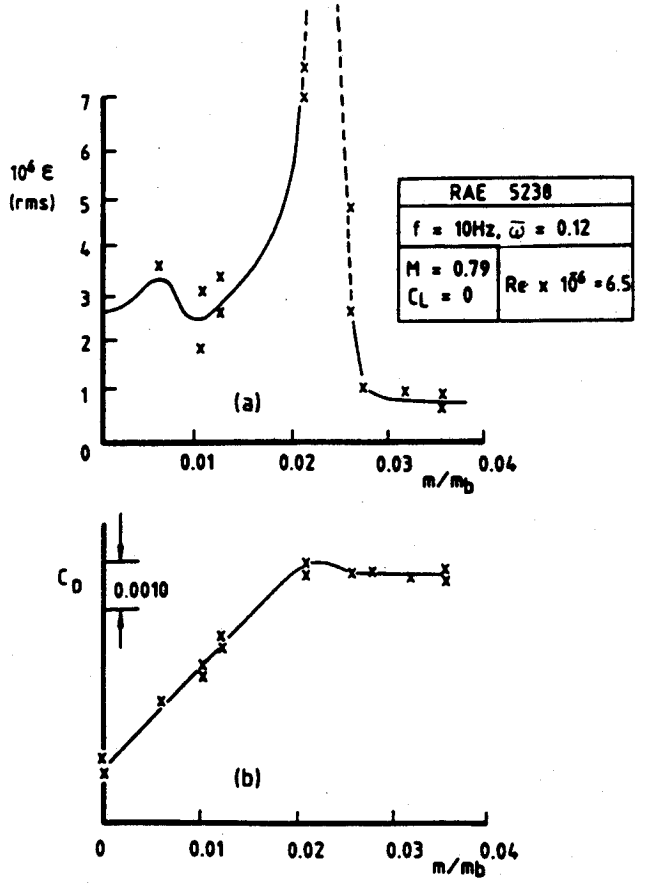

Fig. 10 Variation of unsteady wing-root strain and drag coefficient with air injection ratio.[1]

A potentially very serious problem in regard to dynamic simulation is subscale tests as indicated by the experimental results[1] shown in Fig. 10. Boundary-layer tripping was accomplished by air blowing through perforations at 5% chord. The results in Fig. 10 indicate that when transition is not moved all the way to 5% chord (at blowing rates above $m/m_b \approx 0.027$), the transition effects can become magnified greatly. (How this transition behavior is verified by the drag characteristics in Fig. 10 is discussed in Ref. 1.) For $m/m_b = 0.023$, the bending amplitude became excessive and the blowing rate was increased to $m/m_b = 0.030$, resulting in the damped behavior typical of a turbulent boundary layer (at $\alpha = 0$), as was illustrated in Fig. 2. Figure 10 shows that the bending oscillations reach a maximum for a certain transition location, determined by m/m_b. Why this occurs can be understood when studying the leeside pressure distribution. (Note that even though $\alpha = 0$, the plunging section on the bending wing experiences the effective angle of attack $\bar{\alpha} = \dot{z}/U_\infty$.)

One important parameter that determines the occurence of boundary-layer transition is the local pressure gradient. Other parameters are freestream Reynolds number, freestream turbulence, surface roughness, and, in the present case, surface blowing, which has a roughness-like effect. The moving wall

effect on the oscillating wing (Fig. 9) has to compete with, in particular, the effects of pressure gradients and blowing. The experimental results in Fig. 11 illustrate how the pressure gradient affects transition and the induced wing oscillation.

It is obvious that when transition occurs aft of midchord the plunging-induced moving wall effect is overmatched by the (static) effect of the large adverse pressure gradient. However, forward of midchord the pressure gradients are much milder (see inset in Fig. 11). Thus, the moving wall effect can influence transition sufficiently to generate the observed large bending oscillations only when the blowing rate has been increased to the range $0.020 > m/m_b > 0.025$, which is sufficient to move transition forward of midchord, $\xi_{tr} < 0.5$. When the blowing rate is increased further, $m/m_b > 0.025$, transition moves forward of quarter-chord, $\xi_{tr} > 0.25$, where the moving wall effect is overmatched again, this time by large (static) favorable pressure gradients (see inset in Fig. 11). Consequently, the bending oscillations rapidly decrease in amplitude towards the level obtained for fixed transition (compare Figs. 1 and 11).

The different oscillation amplitudes for the two airfoils at $m/m_b < 0.020$ can be explained if transition (at $Re = 6.5 \times 10^6$) for no blowing occurs forward of three-quarter-chord, $\xi_{tr} < 0.75$, in which case the milder pressure gradient for RAE 5238 compared to RAE 5237 would allow the bending-induced moving wall effect to be more effective, resulting in a larger oscillation amplitude for RAE 5238 than for RAE 5237, in accordance with the experimental results in Fig. 11. Another experimental data trend in Fig. 11, the earlier start (lower m/m_b) and later cessation (larger m/m_b) of the larger amplitude oscillations for RAE 5238 than for RAE 5237, can also be traced to the difference in pressure distributions. That is, the steep adverse pressure gradient extends farther forward from the trailing edge and the steep favorable pressure gradient starts farther away from the leading edge for RAE 5237 than for RAE 5238.

If one compares the experimental results[15] obtained at different Mach numbers, one finds a similar correlation between the pressure (gradient) distribution and the bending response (Fig. 12). Thus, at $M_\infty = 0.8$, where the steep adverse pressure gradient extends further forward than at $M_\infty = 0.5$, a higher blowing rate is needed, $m/m_b > 0.02$ compared to $m/m_b > 0.01$, before transition is moved forward into the shallow pressure gradient region and the large bending response results.

Finally, if the Reynolds number is decreased[15] (Fig. 13), larger blowing rates are required to move transition to a position where the moving wall effects can generate significant transition perturbations, $m/m_b > 0.020$ for $Re = 3.0 \times 10^6$ compared to $m/m_b > 0.015$ for $Re = 6.5 \times 10^6$. As the plunging-induced moving wall effect has to compete with higher blowing rates when transition has reached the shallow pressure gradient region for $Re = 3.0 \times 10^6$ than in the case of $Re = 6.5 \times 10^6$, the induced transition perturbation is reduced greatly, resulting in a greatly reduced bending response. Apparently, at the lower Reynolds number, transition for blowing rates $m/m < 0.02$ is located aft of three-quarter chord, $\xi_{tr} > 0.75$, where the pressure gradient steepens (see inset in Fig. 13), with the result that the bending response is reduced greatly in comparison to the response at $Re = 6.5 \times 10^6$ (Fig. 3). (These results support the assumption made earlier in the discussion of Fig. 11 that transition at $Re = 6.5 \times 10^6$ occurs forward of three-quarter chord, $\xi_{tr} < 0.75$, even in the absence of blowing.)

These results are in complete agreement with the general experience in regard to moving wall effects in both two- and three-dimensional flows.[12] That is, the closer the flow conditions are to the critical one, the higher the potential of the moving wall effect is. Thus, in the present case, it is not the extent of laminar flow that matters but rather how close the free, unperturbed transition is to the shallow pressure gradient region. That is, the problem is not relegated to low Reynolds

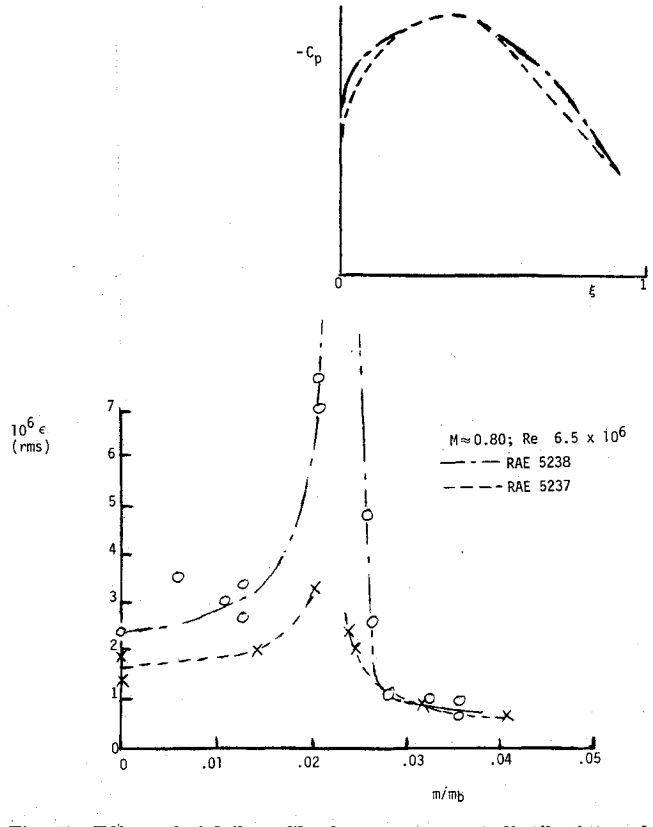

Fig. 11 Effect of airfoil profile shape on pressure distribution and wing bending response.[15]

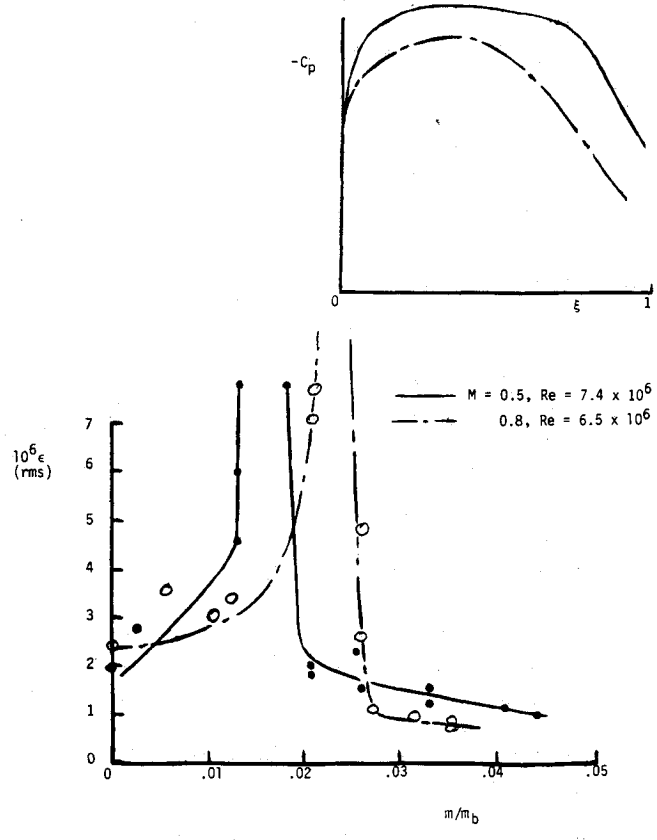

Fig. 12 Effect of Mach number on airfoil pressure distribution and wing bending response.[15]

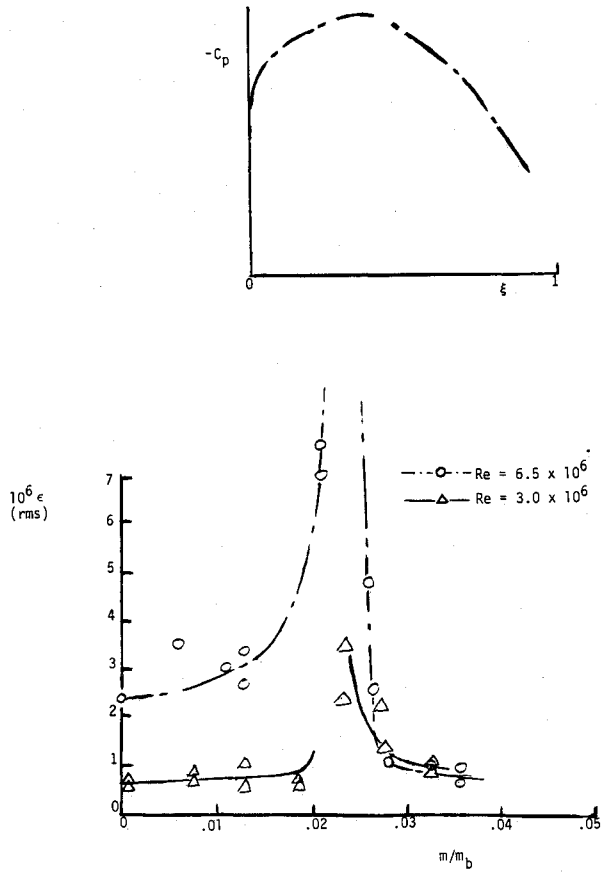

Fig. 13 Effect of Reynolds number and air blowing on wing bending response.[15]

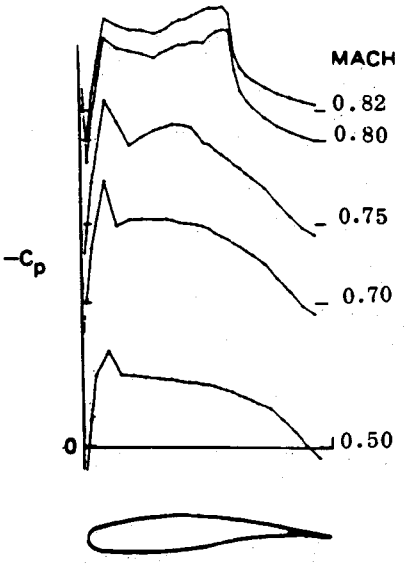

Fig. 14 Effect of Mach number on supercritical airfoil upper side pressure distribution.[19]

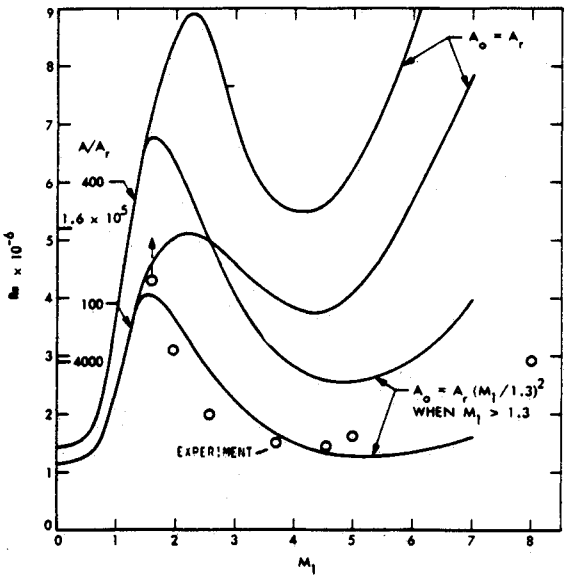

Fig. 15 Flat plate transition as predicted by linear stability theory.[20]

number flows, as on small high-performance gliders, or large transport aircraft with suction to achieve laminar flow, as has been suggested. Quite to the contrary, as Fig. 13 shows, the problem may be less severe in these cases than in higher Reynolds number flows.

The results in Figs. 10–13 illustrate the problem one faces in subscale testing, even when the flow is attached. Similar problems are encountered when testing bodies of revolution,[16–18] although the transition-induced effects in that case usually increase rather than decrease the damping. That supercritical airfoils will experience transition-induced oscillations in bending[3] is to be expected, based upon the pressure distribution results[19] shown in Fig. 14. From the discussion of Figs. 11–13 it is clear that a pressure distribution with a large chord-wise extent of the low-pressure gradient region will be especially sensitive to transition-induced plunging oscillations.

The pressure distributions for the two highest Mach numbers in Fig. 14 show that coupling with plunging oscillations could potentially cause transition to oscillate over half the chord length. Of course, at these Mach numbers compressibility effects become important. However, based upon linear stability analysis results for a flat plate[20] (Fig. 15), one does not expect the effect to become large until the flow becomes supersonic locally. In that case, the strong shock terminating the local supersonic flow region is likely to cause boundary-layer separation, a case beyond the scope of the present paper.

Not surprisingly, the conclusion is the same as before,[2] i.e., *full dynamic simulation* in a wind tunnel test is only possible if the full-scale Reynolds number is reached. Wind tunnels with the needed simulation capability exist,[21,22] and others will undoubtedly become available. However, they will all be in too much demand to be able to accommodate all of the development testing.[23] As there will still be some time before the vehicle designer will be able to get his information from numerical simulation methods, he needs some alternate means for prediction in the meantime. Such means can be provided by the analytic extrapolation method described in Refs. 24 and 25. It should be emphasized, however, that the application of those methods requires a thorough understanding of the flow phenomena involved, which can vary dramatically even for subtle changes in vehicle geometry or test/flight conditions.

Conclusions

An analysis of existing experimental results leads to the following conclusions.

1) The coupling between boundary-layer transition and vehicle motion is strong and can have a large effect on the airfoil dynamics even in the case of attached flow.

2) Great care has to be exercised in the use of subscale wind tunnel test results. Only when the flow phenomena involved are thoroughly understood is it possible to extrapolate analytically to full-scale Reynolds number.

References

[1]Mabey, D. G., Ashill, P. R., and Welsh, B. L., "Aeroelastic Oscillations Caused by Transitional Boundary Layers and Their Attenuation," *Journal of Aircraft*, Vol. 24, July 1987, pp. 463–469.

[2]Ericsson, L. E. and Reding, J. P., "Scaling Problems in Dynamic Tests of Aircraft-like Configurations," Paper 25, AGARD-CP-227, Feb. 1978.

[3]Houvik, R., Kraan, A. N., and Zwaan, R. J., "Wind-Tunnel Study of the Flutter Characteristics of a Supercritical Wing," *Journal of Aircraft*, Vol. 19, May 1982, pp. 400–405.

[4]Greidanus, J. H., van de Vooren, A. I., and Bergh, H., "Experimental Determination of the Aerodynamic Characteristics of an Oscillating Wing with Fixed Axis of Rotation," National Aerospace Laboratories, Netherlands, NLL Rept. F101, 1952.

[5]Ericsson, L. E., "Comment on Aeroelastic Oscillations Caused by Transitional Boundary Layers and Their Attenuation," *Journal of Aircraft*, Vol. 25, Oct. 1988, pp. 975–976.

[6]McCroskey, W. J., McAlister, K. W., Carr, L. W., Pucci, S. L., Lambert, O., and Indergrand, R. F., "Dynamic Stall on Advanced Airfoil Sections," *Journal of the American Helicopter Society*, Vol. 13, Jan. 1981, pp. 40–50.

[7]McCroskey, W. J., and Phillipe, J. J., "Unsteady Viscous Flow on Oscillating Airfoils," *AIAA Journal*, Vol. 13, Jan. 1975, pp. 71-79.

[8]Ericsson, L. E. and Reding, J. P., "Unsteady Flow Concepts for Dynamic Stall Analysis," *Journal of Aircraft*, Vol. 21, Aug. 1984, pp. 601–606.

[9]Ericsson, L. E. and Reding, J. P., "Fluid Mechanics of Dynamic Stall, Part I, Unsteady Flow Concepts," *Journal of Fluids and Structures*, Vol. 2, Jan. 1988, pp. 1–33.

[10]Ericsson, L. E. and Reding, J. P., "Fluid Mechanics of Dynamic Stall, Part II, Prediction of Full Scale Characteristics," *Journal of Fluids and Structures*, Vol. 2, March 1988, pp. 113–143.

[11]Ericsson, L. E. and Reding J. P., "Dynamic Stall of Helicopter Blades," *Journal of the American Helicopter Society*, Vol. 7, Jan. 1972, pp. 10–19.

[12]Ericsson, L. E., "Moving Wall Effects in Unsteady Flow," *Journal of Aircraft*, Vol. 25, Nov. 1988, pp. 977–990.

[13]Swanson, W. M., "The Magnus Effect: A Summary of Investigations to Date," *Journal of Basic Engineering*, Vol. 83, Sept. 1961, pp. 461–470.

[14]Carta, F. O., "A Comparison of the Pitching and Plunging Response of an Oscillating Airfoil," NASA CR-3172, Oct. 1979.

[15]Mabey, D. G. and Ashill, P. R., "On Aeroelastic Oscillations Associated with Transitional Boundary Layers," Royal Aircraft Establishment, UK, TM-Aero 1995, Feb. 1984.

[16]Ericsson, L. E., "Effects of Boundary-Layer Transition on Vehicle Dynamics," *Journal of Spacecraft and Rockets*, Vol. 6, Dec. 1969, pp. 1404–1409.

[17] Ericsson, L. E., "Transition Effects on Slender Vehicle Stability and Trim Charactersitics," *Journal of Spacecraft and Rockets*, Vol. 11, Jan. 1974, pp. 3–11.

[18]Ericsson, L. E., "Viscous Effects on Missile Aerodynamics at Low Angles of Attack," *Journal of Spacecraft and Rockets*, Vol. 18, Sept.–Oct. 1981, pp. 401–405.

[19]den Boer, R. G. and Houvink, R., "Analysis of Transonic Aerodynamic Characteristics for a Supercritical Airfoil Oscillating in Heave, Pitch and with Oscillating Flap," Paper 4, AGARD CP-374, Jan. 1985.

[20]Mack, L. M., "Linear Stability Theory and the Problem of Supersonic Boundary-Layer Transition," *AIAA Journal*, Vol. 13, March 1975, pp. 278–289.

[21]Ohman, L. H., "The NAE High Reynolds Number 15 in. × 60 in. Two-Dimensional Test Facility," National Research Council, Ottawa, Canada, Rept. LTR-HA-4, 1970.

[22]Howell, R. R. and McKinney, L. W., "The U.S. 2.5 Meter Cryogenic High Reynolds Number Tunnel," 10th ICAS Congress, Ottawa, Canada, Oct. 1976.

[23]Baals, D. D., ed., "Workshop on High Reynolds Number Research," NASA SP-2009, 1979.

[24]Ericsson, L. E. and Reding, J. P., "Dynamic Simulation Through Analytic Extrapolation," *Journal of Spacecraft and Rockets*, Vol. 19, No. 2, March–April 1982, pp. 160–166.

[25]Ericsson, L. E. and Reding, J. P., "Analytic Extrapolation to Full-Scale Aircraft Dynamics," *Journal of Aircraft*, Vol. 21, March 1984, pp. 222–224.